

1 Iterated non-Linear Model Predictive Control based on
2 Tubes and Contractive Constraints

3 M.Murillo^{a,*}, G.Sánchez^a, L.Giovanini^a

4 ^a*Research Institute for Signals, Systems and Computational Intelligence, sinc(i),*
5 *FICH-UNL/CONICET, Ciudad Universitaria UNL, 4° piso FICH, (S3000) Santa Fe,*
6 *Argentina.*

7 **Abstract**

8 This paper presents a predictive control algorithm for non-linear systems
9 based on successive linearizations of the non-linear dynamic around a given
10 trajectory. A linear time varying model is then obtained and the non-convex
11 constrained optimization problem is transformed into a sequence of locally
12 convex ones that can be solved using standard quadratic programming tech-
13 niques. The robustness of the proposed algorithm is addressed adding a
14 convex contractive constraint that forces the cost function to remain con-
15 stant or to decrease within the current time instant, determining an upper
16 bound for the performance index. To account for linearization errors and
17 to obtain more accurate results an inner iteration loop is also added to the
18 algorithm. Also, a simple methodology to obtain an outer bounding-tube for
19 state trajectories is presented. The convergence of the iterative process and
20 the stability of the closed-loop system are analysed. The simulation results
21 show the effectiveness of the proposed algorithm in controlling a quadcopter
22 type unmanned aerial vehicle.

23 *Keywords:* contractive constraint, iterative process, non-linear model
24 predictive control, robust model predictive control

*Corresponding author

Email addresses: mmurillo@sinc.unl.edu.ar (M.Murillo),
gsanchez@sinc.unl.edu.ar (G.Sánchez), lgiovanini@sinc.unl.edu.ar (L.Giovanini)

25 **1. Introduction**

26 Model predictive control (MPC) refers to a class of algorithms in which
27 models of the plant are used to predict the future behaviour of the system
28 over a prediction horizon. It is formulated by solving an on-line optimization
29 problem. The optimal control input sequence is calculated by minimizing
30 an objective function subject to constraints. Only the first element of the
31 computed optimal control input is applied to the plant according to a receding
32 horizon strategy [1, 2]. Linear MPC has been successfully applied in a variety
33 of cases due to its ability to explicitly incorporate the system model and
34 state/inputs constraints into the control calculation [3–6].

35 In the last few decades, MPC principles have been extended to non-linear
36 processes yielding to non-linear model predictive control (NMPC). The use
37 of general non-linear programming (NLP) techniques to solve the NMPC
38 problem has been proposed in several works [7–10]. However, the solution
39 methods based on NLP present some drawback. First, these algorithms are
40 computationally demanding, as they require to solve on-line a non-linear
41 optimization problem. Moreover, the constraints introduced by the non-
42 linear model dynamics yields to non-convex optimization problems.

43 Linearization and linear approximation have been adopted in a variety
44 of works to overcome the computational complexity problem [11, 12]. The
45 main advantage of these methods lie in the fact that the model used in the
46 prediction calculation is a set of local linear approximation of the dynamics
47 of the plant, thus converting the non-linear optimization problem into a set
48 of locally convex ones, as it is done in [13–15]. However, linear predictive
49 control techniques do not automatically ensure the stability of the closed-
50 loop system. This issue has been studied by numerous researchers for many
51 years (see [11, 16] for an overview). One way to address the stability problem
52 is to add a contractive constraint to the optimization problem. This idea was
53 firstly introduced by *Yang* and *Polak* [17] and the stability proof was devel-
54 oped by *De Olivera* and *Morari* [18]. In this approach, the authors propose
55 to add a contractive constraint that forces the system states to decrease at
56 each time step. To the best of our knowledge, there are few works that ad-
57 dress the addition of such contractive constraint and also this constraint has
58 only been used to contract the system states.

59 In this paper we present a novel robust predictive control algorithm for
60 non-linear systems. The proposed algorithm uses a linearization process
61 along pre-defined trajectories that transform the non-convex optimization

62 problem into a set of locally convex ones, which can be solved using the
 63 standard quadratic programming (QP) techniques. Here, to address stabil-
 64 ity and convergence issues, the addition of a set of contractive constraints to
 65 the optimization problem is analysed. These constraints force the cost func-
 66 tions to decrease or (at least) to remain constant within the current time
 67 instant, thus allowing to take into account disturbances and determining an
 68 upper bound of the cost functions value. Moreover, an inner iteration loop
 69 is added to the proposed algorithm to account for linearization errors and to
 70 obtain more accurate results.

71 The organization of this paper is as follows: in Section 2 the formulation
 72 of the NMPC algorithm with the addition of the contractive constraint is
 73 presented. In Section 3 a simple methodology to obtain an outer bounding-
 74 tube for state trajectories is analysed. In Section 4 an inner iteration loop is
 75 added to the previous algorithm. Simulation results are shown in Section 5.
 76 Finally, conclusions are discussed in Section 6.

77 2. Non-linear Model Predictive Control Formulation

78 Consider the discrete non-linear system

$$79 \quad x_{k+1} = f(x_k, u_k, d_k) \quad (1)$$

80 where $x_k = x(k) \in \mathfrak{R}^n$, $u_k = u(k) \in \mathcal{U} \subseteq \mathfrak{R}^m$ and $d_k = d(k) \in \mathcal{D} \subseteq \mathfrak{R}^l$
 81 are the state vector, the control input vector and the bounded disturbance
 82 vector, respectively, \mathcal{U} is the input constraint set and $f(\cdot)$ is a continuous
 83 and differentiable vector function that describes the dynamics of the system.

84 The non-linear model predictive control problem is formulated as a regu-
 85 latory problem stated as follows:

86 For a given¹ disturbance sequence

$$87 \quad \mathbf{d}_k = [d_{k|k}, \dots, d_{k+N-1|k}]^T, \quad (2)$$

88 find at each time instant k , a control input sequence

$$89 \quad \mathbf{u}_k = [u_{k|k}, \dots, u_{k+N-1|k}]^T, \quad (3)$$

¹If \mathbf{d}_k is not available, the most common assumption is $\mathbf{d}_{k+i} = \mathbf{d}_{k+i-1}$, $i = 1, \dots, N$

90 and predicted state sequence

$$91 \quad \mathbf{x}_k = [x_{k+1|k}, \dots, x_{k+N|k}]^T, \quad (4)$$

92 over a prediction horizon of N sampling intervals, such that

$$93 \quad \begin{aligned} & \min_{\mathbf{u}_k \in \mathcal{U}} \mathcal{J}(k) \\ & \text{st. } x_{k+1} = f(x_k, u_k, d_k). \end{aligned} \quad (5)$$

94 The vectors $d_{k+i|k}$, $u_{k+i|k}$ and $x_{k+i|k}$ in Eqs. (2) to (4) represent the distur-
 95 bance, input and state vectors at time $k+i$ that are predicted using the
 96 information available at time k .² The optimal solution of the problem (5) is
 97 denoted here as:

$$98 \quad \mathbf{u}_k^* = [u_{k|k}^*, \dots, u_{k+N-1|k}^*]^T. \quad (6)$$

99 Regardless the cost function $\mathcal{J}(k)$ is convex or not, the optimization
 100 problem (5) is non-convex due to the non-linearity of the system dynamics,
 101 and the computational effort is a major issue in its on-line implementation. If
 102 $\mathcal{J}(k)$ is chosen to be a quadratic cost function, then the convexity of (5) can
 103 be recovered by approximating the non-linear model (1) with a linear time-
 104 varying (LTV) one [19, 20], which can be obtained linearizing the system
 105 around a desired state and input trajectory \mathbf{x}_k^r , \mathbf{u}_k^r , where

$$106 \quad \mathbf{x}_k^r = [x_{k+1|k}^r, \dots, x_{k+N|k}^r]^T, \quad (7)$$

107 and

$$108 \quad \mathbf{u}_k^r = [u_{k|k}^r, \dots, u_{k+N-1|k}^r]^T. \quad (8)$$

109 Assuming that a reference perturbation $d_{k+i|k}^r$, $i = 0, \dots, N-1$ is given
 110 or estimated, then the dynamic behavior of the deviation from the desired
 111 trajectory can be written as an LTV model

$$112 \quad \tilde{x}_{k+1|k} = A_{k|k} \tilde{x}_{k|k} + B_{u_{k|k}} \tilde{u}_{k|k} + B_{d_{k|k}} \tilde{d}_{k|k}, \quad (9)$$

113 where

$$114 \quad \tilde{x}_{k|k} = x_{k|k} - x_{k|k}^r, \quad \tilde{u}_{k|k} = u_{k|k} - u_{k|k}^r \quad \text{and} \quad \tilde{d}_{k|k} = d_{k|k} - d_{k|k}^r. \quad (10)$$

²When it clearly refers to current time k , the time dependency at which the information is available will be omitted, i.e. $(\cdot)_{k+i|k} = (\cdot)_{k+i}$

115 The matrices $A_{k|k}$, $B_{u_{k|k}}$ and $B_{d_{k|k}}$, are the Jacobian matrices of the discrete
 116 non-linear system (1), and they are defined as follows

$$A_{k|k} = \left. \frac{\partial f(x_k, u_k, d_k)}{\partial x_k} \right|_{(*)}, \quad B_{u_{k|k}} = \left. \frac{\partial f(x_k, u_k, d_k)}{\partial u(k)} \right|_{(*)}, \quad B_{d_{k|k}} = \left. \frac{\partial f(x_k, u_k, d_k)}{\partial d(k)} \right|_{(*)}, \quad (11)$$

117 where $(*)$ stands for (x_k^r, u_k^r, d_k^r) . In terms of the LTV system (9), the fol-
 118 lowing quadratic objective function $\mathcal{J}(k)$, commonly used in the literature,
 119 is adopted:
 120

$$121 \quad \mathcal{J}(k) = \sum_{i=0}^{N-1} \left[\tilde{x}_{k+i|k}^T Q \tilde{x}_{k+i|k} + \tilde{u}_{k+i|k}^T R \tilde{u}_{k+i|k} \right] + \tilde{x}_{k+N|k}^T P_{k|k} \tilde{x}_{k+N|k}, \quad (12)$$

122 where $Q, R, P_{k|k}$ are positive definite matrices; $P_{k|k}$ is the terminal weight
 123 matrix that is chosen so as it satisfies the Lyapunov equation

$$124 \quad P_{k|k} - A_{k|k}^T P_{k|k} A_{k|k} = Q. \quad (13)$$

125 As a result, the non-convex optimization problem (5) can be rewritten as
 126 a convex optimization problem as follows:

$$127 \quad \begin{aligned} & \min_{\tilde{\mathbf{u}}_k \in \mathcal{U}} \mathcal{J}(k) \\ \text{st.} \quad & \begin{cases} \tilde{x}_{k+1|k} = A_{k|k} \tilde{x}_{k|k} + B_{u_{k|k}} \tilde{u}_{k|k} + B_{d_{k|k}} \tilde{d}_{k|k}, \\ \tilde{x}_{k|k} = x_{k|k} - x_{k|k}^r, \\ \tilde{u}_{k|k} = u_{k|k} - u_{k|k}^r, \\ \tilde{d}_{k|k} = d_{k|k} - d_{k|k}^r. \end{cases} \end{aligned} \quad (14)$$

128 In Algorithm 1 the NMPC receding horizon control technique is summarized.

Algorithm 1: NMPC Algorithm

Given $Q, R > 0$, $x_{k|k}$ the initial condition.

Step 1: Obtain the linearization trajectory $\mathbf{x}_k^r, \mathbf{u}_k^r$ using as initial condition $\mathbf{u}_k^0 = [u_{k|k-1}^*, u_{k+1|k-1}^*, \dots, u_{k+N-2|k-1}^*, 0]^T$ and estimate d_{k+i} for $i = 0, \dots, N - 1$

Step 2: Obtain the LTV system (9) and $P_{k|k}$ solving (13)

Step 3: Compute the optimal control input sequence $\tilde{\mathbf{u}}_k^*$ solving (14)

Step 4: Update $\mathbf{u}_k^* \leftarrow \mathbf{u}_k^r + \tilde{\mathbf{u}}_k^*$

Step 5: Apply $u_{k|k} = u_{k|k}^*$ to the system

Step 6: Move the horizon forward to the next sampling instant $k \leftarrow k + 1$ and go back to **Step 1**

129
130 Linearization techniques are the most straightforward ways to adapt linear
131 control methods to non-linear control problems. In absence of perturbations
132 and linearization errors, the Algorithm 1 will guarantee the closed-loop
133 stability.

134 **Assumption 1.** The LTV system (9) is stabilizable for $\mathbf{u}_k \in \mathcal{U}$.

135 **Assumption 2.** The prediction horizon N is chosen sufficiently long.

136 **Assumption 3.** There are no perturbations, i.e. $d_{k+i} = 0, i = 0, \dots, N - 1$.

137

138 **Theorem 1.** *Let assumptions 1 - 3 hold. If the optimization problem (14)*
139 *solved using Algorithm 1 is feasible, then the origin is an exponentially stable*
140 *equilibrium point.*

141 *Proof.* See Appendix 8.A. □

142 Although assumption 1 establishes that the prediction horizon N should
143 be long enough, for engineering applications this horizon should be actually
144 chosen as small as possible in order to reduce the workload of online calcu-
145 lation. Consequently, the stability of the system should be ensured using a
146 different argument (see for instance [15, 16, 18]). Moreover, if disturbances
147 are present Theorem 1 might not be satisfied because the contractivity of

148 the cost function cannot be guaranteed at the successive time instants. To
 149 address this problem, we propose to add the convex contractive constraint

$$150 \quad \mathcal{J}(k) \leq \mathcal{J}_0(k), \quad (15)$$

151 to the optimization problem (14), where $\mathcal{J}_0(k)$ denotes the cost function
 152 evaluated for the initial solution

$$153 \quad \mathbf{u}_k^0 = [u_{k|k-1}^*, u_{k|k-1}^*, \dots, u_{k+N-2|k-1}^*, 0]^T. \quad (16)$$

154 at iteration k . Note that this constraint forces the cost function to remain
 155 constant or to decrease within the current time instant, thus determining an
 156 upper bound for $\mathcal{J}(k)$. Then, the new optimization problem can be stated
 157 as follows:

$$158 \quad \begin{aligned} & \min_{\tilde{\mathbf{u}}_k \in \mathcal{U}} \mathcal{J}(k) \\ \text{st.} \quad & \begin{cases} \tilde{x}_{k+1|k} = A_{k|k} \tilde{x}_{k|k} + B_{k|k} \tilde{u}_{k|k}, \\ \tilde{x}_{k|k} = x_{k|k} - x_{k|k}^r, \\ \tilde{u}_{k|k} = u_{k|k} - u_{k|k}^r, \\ \mathcal{J}(k) \leq \mathcal{J}_0(k). \end{cases} \end{aligned} \quad (17)$$

159 As the contractive constraint (15) is defined at the current time instant, if
 160 any perturbation occur the value of $\mathcal{J}(k)$ can increase (only at time k) but
 161 then it is forced to decrease or to remain constant. The optimization problem
 162 (17) can be seen as a multi-objective problem, where the constraint (15) is
 163 used to guarantee the stability of the closed-loop system and $\mathcal{J}(k)$ is used to
 164 measure the performance of the closed-loop system.

165 **Theorem 2.** *If the optimization problem (17) solved using Algorithm 1 is*
 166 *feasible, then the closed-loop system is stable.*

167 *Proof.* See Appendix 8.B. □

168 **Remark 1.** Note that in the absence of perturbations, the constraint (15)
 169 guarantees the contractivity of the cost function at successive time instants,
 170 i.e.

$$171 \quad \mathcal{J}^*(k) \leq \mathcal{J}(k) \leq \mathcal{J}_0(k) \leq \mathcal{J}^*(k-1) \leq \mathcal{J}(k-1). \quad (18)$$

172 **Remark 2.** As the stability of the system is guaranteed, the prediction
 173 horizon N can be reduced, consequently lowering the workload of online
 174 calculation (see for instance the simulation example of Section 5.1).

175 **Remark 3.** The addition of the constraint (15) is equivalent to the addition
 176 of an input constraint on \mathbf{u}_k , hence if the system is stabilizable with $\mathbf{u}_k \in \mathcal{U}$,
 177 then the initial feasibility is guaranteed and using the argument of recursive
 178 feasibility, the contractive constraint (15) does not affect original feasibility
 179 [16].

180 3. Robust Non-linear Model Predictive Control

181 The design of robust control algorithms have been studied for many years
 182 because such algorithms have the ability to handle system parametric and
 183 structural uncertainties (modeled as bounded disturbances) during the sys-
 184 tem operation. One possible way of accounting for robustness in NMPC
 185 algorithm consists in evaluating at each sampling instant all the possible
 186 system state trajectories for a given (or estimated) disturbance. This can
 187 be done solving an optimization problem that considers the different states
 188 trajectories, i.e.:

$$\begin{aligned}
 & \min_{\tilde{\mathbf{u}}_k^l \in \mathcal{U}} \mathcal{J}(k) \\
 \text{st. } & \begin{cases} \tilde{x}_{k+1|k}^l = A_{k|k}^l \tilde{x}_{k|k}^l + B_{k|k}^l \tilde{u}_{k|k}^l, \\ \tilde{x}_{k|k}^l = x_{k|k}^l - x_{k|k}^r, \\ \tilde{u}_{k|k}^l = u_{k|k}^l - u_{k|k}^r, \\ \mathcal{J}^l(k) \leq \mathcal{J}_0^l(k), \end{cases} \quad (19)
 \end{aligned}$$

190 where $l = 1, \dots, m$ stands for the different system realizations regarding the
 191 given disturbance. As a result, it can be thought that each state trajectory
 192 defines an edge of a time varying polytope [21, 22]. This polytope can be used
 193 to generate a tube which actually contains all the possible state trajectories.
 194 Tubes have been widely used to bound uncertainties [21, 23–25]. However,
 195 the determination of an exact tube for non-linear systems is very difficult.

196 In this work, the LTV system (9) is obtained by a first order Taylor
 197 series expansion. To measure the deviation between the LTV system and
 198 the non-linear one, the second order Taylor remainder is used to bound these
 199 linearization errors. Instead of obtaining the sequence of all state trajectories
 200 \mathbf{x}_k^l , $l = 1, \dots, m$, we propose to use the Taylor remainder to compute state
 201 trajectory sequence with the worst uncertainty \mathbf{x}_k^Δ . This trajectory can then
 202 be used to determine an outer bounding-tube that contains all the state
 203 trajectories. Finally, this tube is used to guarantee the stability of the closed-
 204 loop system. The proposed procedure is explained below.

205 The non-linear system (1) can be approximated exactly with an LTV
 206 model if the second order Taylor reminder $R_1(\tilde{x}_k, \tilde{u}_k, \tilde{d}_k)$ ³ is added to the
 207 RHS of (9)

$$208 \quad \tilde{x}_{k+1|k} = A_{k|k}\tilde{x}_{k|k} + B_{k|k}\tilde{u}_{k|k} + R_1(\tilde{x}_k, \tilde{u}_k, \tilde{d}_k). \quad (20)$$

209 From equation (20) it can be seen that the term $R_1(\cdot)$ acts as an additive
 210 disturbance. This term can be maximized⁴ in order to obtain \mathbf{x}_k^Δ , which is the
 211 state trajectory sequence with the worst uncertainty. Once \mathbf{x}_k^Δ is obtained,
 212 its associated cost $\mathcal{J}^\Delta(k)$ can be computed. Then, the stability condition
 213 for the whole problem can be established if this cost function is forced to
 214 decrease. This can be done adding the following contractive constraint

$$215 \quad \mathcal{J}^\Delta(k) \leq \mathcal{J}_0^\Delta(k), \quad (21)$$

216 to the optimization problem (17). Finally the proposed robust control prob-
 217 lem to be solved is

$$218 \quad \begin{aligned} & \min_{\tilde{\mathbf{u}}_k \in \mathcal{U}} \mathcal{J}(k) \\ \text{st.} \quad & \begin{cases} \tilde{x}_{k+1|k} = A_{k|k}\tilde{x}_{k|k} + B_{k|k}\tilde{u}_{k|k}, \\ \tilde{x}_{k|k} = x_{k|k} - x_{k|k}^r, \\ \tilde{u}_{k|k} = u_{k|k} - u_{k|k}^r, \\ \mathcal{J}(k) \leq \mathcal{J}_0(k), \\ \mathcal{J}^\Delta(k) \leq \mathcal{J}_0^\Delta(k), \end{cases} \end{aligned} \quad (22)$$

219 where $\mathcal{J}_0^\Delta(k)$ denotes the cost functions $\mathcal{J}^\Delta(k)$ evaluated for the initial con-
 220 dition \mathbf{u}_k^0 .

221 By including the contractive constraint (21) the stability of the origin is
 222 guaranteed as $\mathcal{J}^\Delta(k)$ is forced to decrease (or to remain constant). Moreover,
 223 as $\mathcal{J}^\Delta(k)$ is pushed to zero it actually contract the nominal cost. Following
 224 similar arguments as that used in the proof of Theorem 2 and in (18), it can
 225 be shown that if the optimization problem (22) solved using Algorithm 1 is
 226 feasible, then the origin is an exponentially stable equilibrium point.

227 **Remark 4.** Note that as $\mathcal{J}_0^\Delta(k)$ is a relaxed upper bound (see for instance
 228 Figs. 2(c) and 4(b)), then it is surely bigger than $\mathcal{J}^\Delta(k)$, thus not affecting
 229 the feasibility of the optimization problem (22).

³ $R_1(\cdot)$ can be obtained as in [26]

⁴If there is no information about \mathbf{d}_k a given value can be assumed

230 **Remark 5.** Following the same arguments used in **Remark 3**, it can be de-
 231 duced that the addition of the contractive constraint (21) in the optimization
 232 problem (22) does not affect original feasibility.

233 It is worth comparing the proposed approach with those described in [24]
 234 and [21]. In our work an outer bounding-tube is obtained by simply max-
 235 imizing $R_1(\tilde{x}_k, \tilde{u}_k, \tilde{d}_k)$ and then computing the state trajectory \mathbf{x}_k^Δ . Within
 236 this bounding-tube lie all the perturbed system trajectories [23, 27]. Ad-
 237 ditionally, the stability condition is guaranteed just by the inclusion of the
 238 constraint (21). The procedure proposed in [24] by Cannon *et al.* is more
 239 complex. The authors solve a multi-parametric optimization problem with
 240 many constraints yielding a high computational burden (even for a simple
 241 state-space model) and the impossibility to solve the algorithm in real time.
 242 On the other hand, in [21] Langson *et al.* propose a method for robust
 243 MPC of linear constrained systems with uncertainties. They use (convex)
 244 compact polytopes and (convex) closed polyhedrons, which are difficult to
 245 handle when there are several resulting regions. Moreover, the tube is defined
 246 as a sequence of sets of states and associated time-varying control input law.
 247 This is time demanding as they compute all the possible state trajectories to
 248 define the tube.

249 4. Iterated Robust Non-linear Model Predictive Control

250 When non-linear systems are linearized, linearization errors may appear
 251 and they could be large if linearization trajectories are far from the system
 252 operating point. To account for these errors, we propose to include an iter-
 253 ative technique [15, 28] in Algorithm 1 in order to improve the performance
 254 of the closed-loop system. The proposed iteration works as follows: at each
 255 sampling instant, the non-linear system is linearized along a predefined lin-
 256 earization trajectory. The optimal control input sequence is computed and
 257 then it is checked if the breaking loop condition is satisfied. If it is not the
 258 case, the linearization trajectory is re-computed using the new control input
 259 sequence. The non-linear system is re-linearized and the control input se-
 260 quence is re-computed. This loop is followed until the convergence condition
 261 is satisfied. As a result, a more accurate optimal control input sequence \mathbf{u}_k^*
 262 is then obtained. In Algorithm 2 the proposed iterated robust NLMPC tech-
 263 nique is summarized.

Algorithm 2: Iterated Robust NMPC Algorithm

Given $Q, R > 0$, $x_{k|k}$ the initial condition, q the iteration index.

Step 1: Initialize $\mathbf{u}_k^q = [u_{k|k-1}^*, u_{k+1|k-1}^*, \dots, u_{k+N-2|k-1}^*, 0]^T$

Step 2: Obtain the linearization trajectory $\mathbf{x}_k^q, \mathbf{u}_k^q$

Step 3: Obtain the LTV system (9) and $P_{k|k}^q$ solving (13)

Step 4: Compute the optimal control input sequence $\tilde{\mathbf{u}}_k^{*,q}$ solving (22)

Step 5: Update $\mathbf{u}_k^{*,q} \leftarrow \mathbf{u}_k^q + \tilde{\mathbf{u}}_k^{*,q}$

264 **Step 6:** *if* $\|\mathbf{u}_k^{*,q} - \mathbf{u}_k^{*,q-1}\|_\infty \leq \epsilon$

$$\mathbf{u}_k^* \leftarrow \mathbf{u}_k^{*,q},$$

$$k \leftarrow k + 1$$

$$q \leftarrow 0$$

else

$$q \leftarrow q + 1$$

$$\text{Update } \mathbf{u}_k^q = \mathbf{u}_k^{*,q-1}$$

Go back to **Step 2**

end

Step 7: Apply $u_{k|k} = u_{k|k}^*$ to the system and go back to **Step 1**

265 As the optimization problem to be solved in Algorithm 2 includes the
266 contractive constraints (15) and (21), the stability of the algorithm is guar-
267 anteed. Consequently, the iteration process can be stopped at any time, thus
268 improving the online computational burden.

269 **Theorem 3.** *The iteration loop of Algorithm 2 converges to the optimal*
270 *value.*

271 *Proof.* See Appendix 8.C. □

272 5. Simulation Examples

273 In this section simulation examples are shown. Using the quadcopter
274 model described in Appendix D and the iterated robust NMPC technique
275 of Section 4 two autonomous maneuvers are performed. To evaluate the
276 performance of the proposed controller, simulations with different horizons
277 are also performed.

278 *5.1. First Example: Climbing Up, Moving Forward and Landing with Colored*
 279 *Wind Gusts*

280 The first maneuver to be tested is the following: first the quadcopter
 281 starts climbing up with an altitude rate $\dot{h} = 0.15$ [m/sec]. At approximately
 282 $t = 10$ [sec], the vehicle starts moving forward along the x -axis. When $t =$
 283 20 [sec], the quadcopter reaches the desired altitude $h_{sp} = 3$ [m] and it keeps
 284 moving forward for about 5 seconds longer. When $t = 25$ [sec], the vehicle
 285 starts a landing maneuver. Finally, after 10 seconds, the quadcopter is back
 286 in the ground. It is assumed that the quadcopter flies immersed in colored
 287 wind. The forces generated by these wind gusts act at the quadcopter CG
 288 position and they vary randomly between -1.0 [N] and 1.0 [N], as it can be
 seen in Figure 1:

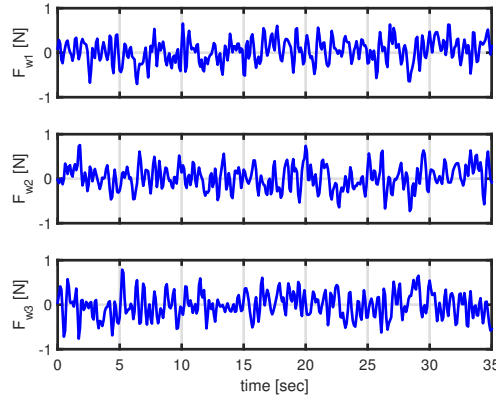


Figure 1: Evolution of colored wind gusts

289 The robust NMPC controller was designed using an horizon $N = 3$ and
 290 sampling period $T_s = 0.1$ [sec]. The weight matrices Q , R and $P_{k|k}$ were
 291 defined as
 292

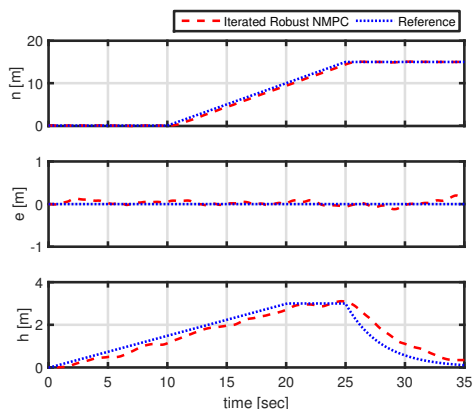
$$Q = \text{diag}(10, 1, 100, 10, 0, 10, 0, 10, 0, 10, 0, 10) \tag{23}$$

$$R = \text{diag}(0.1, 0.1, 0.1, 0.1)$$

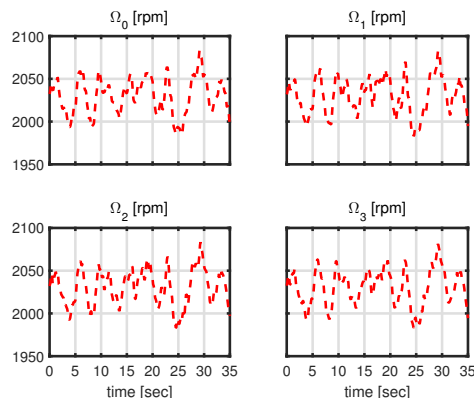
293 while $P_{k|k}$ was computed at each sampling interval using (13). Fig. 2(a)
 294 shows the quadcopter position⁵. It can be seen that the vehicle starts climb-
 295 ing while moving forward. It reaches the desired altitude and continues
 296

⁵The x -axis points to the north (n), the y -axis points to the east (e) and the z -axis points down ($h=-z$)

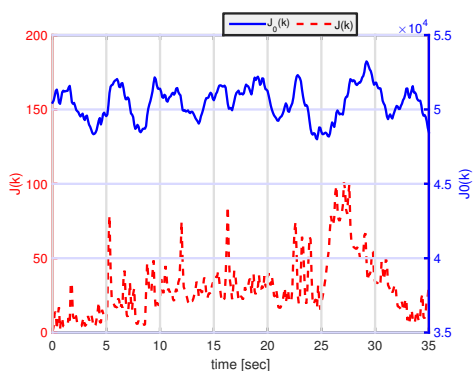
297 moving along the positive x -axis. Finally, it lands in the ground successfully.
 Fig. 2(b) depicts the evolution of the computed optimal control inputs. The



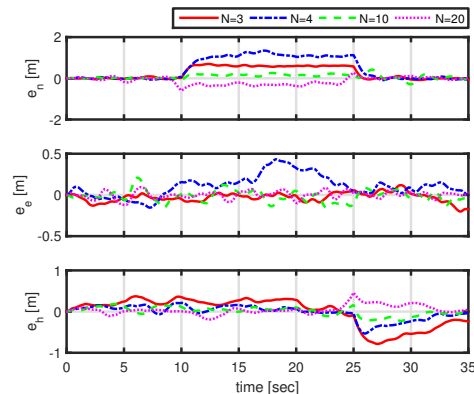
(a) Quadcopter position



(b) Quadcopter control inputs



(c) Evolution of $\mathcal{J}(k)$ with initial guess $\mathcal{J}_0(k)$ for $N = 3$



(d) Position errors for different horizons

Figure 2: Climbing up, moving forward and landing maneuver with colored wind gusts

298
 299 obtained values are physically realizable for a quadcopter. Also, the varia-
 300 tion of the four control inputs are similar in shape and in magnitude, which
 301 allow to maintain the quadcopter at a stable flight. From Fig. 2(c) it can be
 302 seen clearly that the proposed contractive constraint $\mathcal{J}_0(k)$ acts as an upper
 303 bound for the cost function $\mathcal{J}(k)$. This constraint is never active because
 304 the aim of including $\mathcal{J}_0(k)$ in (22) is to limit the searching space of optimal
 305 solutions. It should be noted that despite the value of N was very short,
 306 the proposed maneuver was performed successfully. The adopted value in

307 fact corresponds to shortest horizon possible that can be used in a receding
 308 horizon control scheme with this quadcopter model (the number of unstable
 309 modes plus one [29]). Fig. 2(d) shows the errors in the quadcopter position
 310 when larger values of N are used. As it can be seen, the differences between
 311 the simulations are small. This is very advantageous as the computational
 312 burden of the robust NMPC scheme is reduced if shorter horizons are used.

313 5.2. Second Example: Spiral Motion with Controlled Yaw Angle

314 The second maneuver to be tested is a spiral descend motion with controlled
 315 yaw angle. For this case, the robust NMPC controller was also designed
 316 using an horizon $N = 3$ and sampling period $T_s = 0.1$ [sec]. The
 317 weight matrices Q , R and $P_{k|k}$ were defined as

$$318 \quad \begin{aligned} Q &= \text{diag}(100, 1, 100, 10, 0, 10, 0, 10, 0, 10, 0, 10) \\ R &= \text{diag}(0.1, 0.1, 0.1, 0.1) \end{aligned} \quad (24)$$

319 while $P_{k|k}$ was computed at each sampling interval using (13).

320 The proposed maneuver, in addition of the spiral descend motion, also
 321 controls the quadcopter yaw angle in such a way that the quadcopter x -axis
 322 is always aligned with the circumference radius, and as a result the vehicle
 323 always ‘looks’ at the center of the spiral. This maneuver would result very
 324 useful, for example, if one would use a quadcopter with a fixed-mounted camera
 325 to inspect a tower. As it can be seen in Fig. 3, the desired maneuver was
 326 performed successfully. The quadcopter achieved the spiral descend motion
 327 while the *yaw* angle was controlled in order the quadcopter ‘looks’ at the
 328 center of the spiral. Fig. 4(a) shows the evolution of the computed control
 329 inputs. It can be seen that the propellers which are opposite to each other
 330 have a similar variation. Control inputs practically vary at the beginning
 331 and at the end of the maneuver, staying constant while the quadcopter is
 332 performing the spiral descent. Fig. 4(b) depicts both the cost function
 333 $\mathcal{J}(k)$ and its upper bound $\mathcal{J}_0(k)$. It shows that when the spiral descend is
 334 being performed, the cost is constant and when the quadcopter reaches the
 335 ground, $\mathcal{J}(k)$ effectively tends to zero.

336 5.3. Comparison between iterated robust NMPC and classical NMPC techniques

337
 338 Here, the proposed iterated robust NMPC technique is compared with
 339 the classical NMPC technique presented in [28]. To test the performance

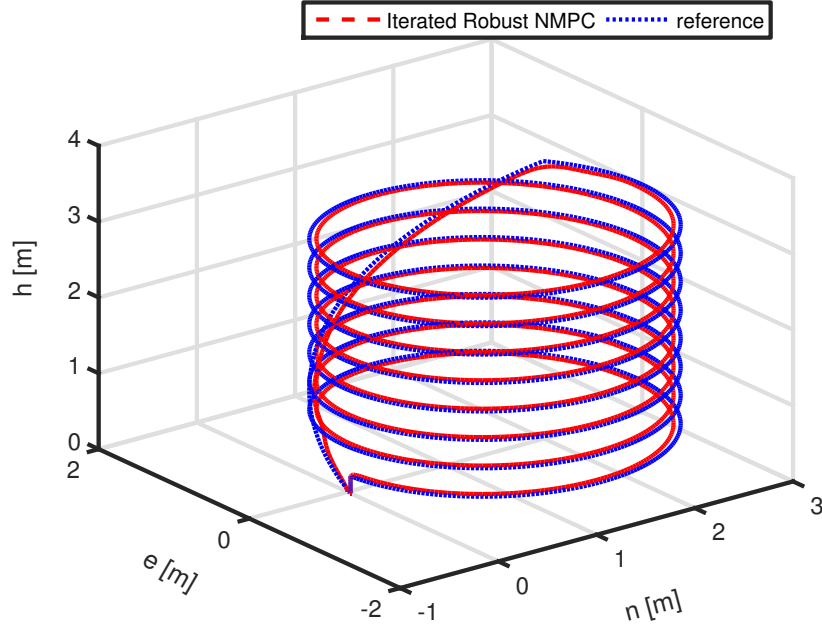
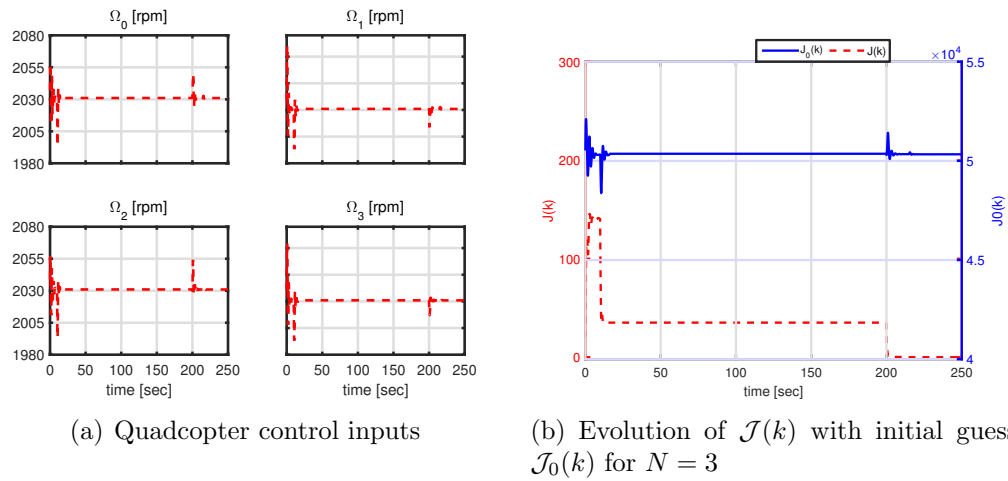


Figure 3: Evolution of the quadcopter position



(a) Quadcopter control inputs

(b) Evolution of $\mathcal{J}(k)$ with initial guess $\mathcal{J}_0(k)$ for $N = 3$

Figure 4: Spiral motion with controlled yaw angle

340 of our algorithm, we simulated the maneuver presented in Section 5.1 using
 341 both algorithms. In Figure 5 it can be seen the errors in the quadcopter
 342 position. The results suggest that when the value of N is maintained and
 343 the contractive constraints are not added to the optimization problem, then
 344 the errors in the quadcopter position are increased. However, in order to ob-
 345 tain a similar response as the one obtained with the iterated robust NMPC,
 346 we had to use the NMPC technique with a larger value of N , thus increas-
 347 ing the online computational workload. On the other hand, the proposed
 348 algorithm could be executed within a maximum of three iterations but as
 349 the stability of the closed-loop system is guaranteed, the iteration loop could
 350 have been stopped with fewer iterations, thus reducing even more the online
 computational workload.

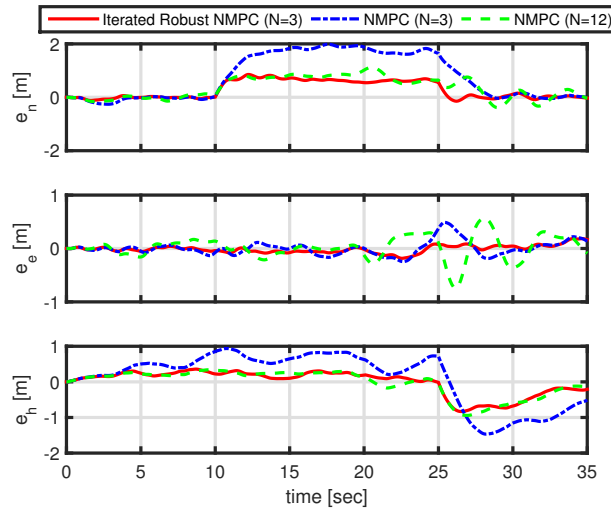


Figure 5: Comparison with the standard NMPC technique

351 Additionally, we have also compared our algorithm with the one proposed
 352 by *Cannon et al.* [24]. We performed the same maneuver as before using
 353 both algorithms. Similar results were obtained when a large horizon was used
 354 with Cannon's algorithm. Moreover, we found that the online computational
 355 burden for this algorithm is three or four times higher than that obtained
 356 with our algorithm.

358 Consequently, because of the presented results the iterated robust NMPC
 359 algorithm may be an useful tool for real time simulations as it allows to obtain
 360 acceptable responses at lower computational burden.

361 6. Conclusion

362 In this paper, a robust non-linear model predictive control technique was
363 presented. The proposed technique is based on the linearization of non-linear
364 systems along pre-defined state trajectories and the minimization of a con-
365 strained objective function. To guarantee the stability of the closed-loop
366 system we add to the optimization problem a contractive constraint that
367 forces the cost function to decrease (or to remain constant) at the current
368 time instant. This stability can be also guaranteed even with uncertainties.
369 As the stability of the system is guaranteed, the inclusion of this constraint
370 allows to reduce the prediction horizon to its minimum value, thus lowering
371 the computational workload. This may be useful when controlling non-linear
372 systems with fast dynamics such as a quadcopter. The robustness of the
373 proposed NMPC algorithm is achieved by using the Taylor reminder to com-
374 pute the state trajectory associated to the worst uncertainty. This trajectory
375 can then be used to determine an outer bounding-tube that contains all the
376 system state trajectories. The proposed methodology to obtain the outer
377 bounding-tube for state trajectories seems to be simpler and less computa-
378 tionally demanding. To account for linearization errors and to improve the
379 performance of the closed-loop system we have included an iteration loop in
380 the robust NMPC algorithm, yielding to the iterated robust NMP algorithm.

381 The iterated NMPC algorithm was used as a central unit that can control
382 a full quadcopter model without the need of decoupling the non-linear sys-
383 tem. To evaluate the performance of this algorithm, we have performed the
384 simulation of two autonomous maneuvers, which were performed both suc-
385 cessfully. Also, the results were compared with those obtained using larger
386 horizons, having no significant differences between the short horizon adopted
387 and the larger ones. Finally, we have performed a comparison between it-
388 erated robust NMPC algorithm and classical NMPC. The results obtained
389 suggest that the proposed algorithm can achieve a similar response to the
390 classical NMPC but using a shorter prediction horizon, thus having a lower
391 computational workload than classical NMPC.

392 7. Acknowledgments

393 The authors wish to thank the *Universidad Nacional de Litoral* (with
394 CAID 501201101 00529 LI) and the *Consejo Nacional de Investigaciones*
395 *Científicas y Técnicas* (CONICET) from Argentina, for their support.

396 **8. Appendices**

397 **A. Proof of Theorem 1**

398 *Proof.* First it is shown that the input and the state converge to the origin,
 399 and then it will be shown that the origin is an stable equilibrium point for
 400 the close-loop system. The combination of convergence and stability gives
 401 asymptotic stability.

402 *Convergence.* Convergence of the state and input to the origin can be estab-
 403 lished by showing that the sequence of cost values is non-increasing.

404 Let the cost function $\mathcal{J}(k)$ be given by (12), with Q , R and $P_{k|k}$ positive
 405 definite matrices; $P_{k|k}$ satisfies the Lyapunov equation.

406 Let $\mathbf{u}_k^* = [u_{k|k}^*, u_{k+1|k}^*, \dots, u_{k+N-1|k}^*]^T$ be the optimal control input se-
 407 quence computed at time k . Assuming that only exists inputs constraints,
 408 then the control input sequence $\hat{\mathbf{u}}_{k+1} = [u_{k+1|k}^*, u_{k+2|k}^*, \dots, u_{k+N-1|k}^*, 0]^T$ is
 409 feasible at time $k+1$. As $P_{k|k}$ satisfies the Lyapunov equation, then the cost
 410 function (12) approximates exactly the infinite cost problem. Then, evaluat-
 411 ing $\mathcal{J}(k)$ for both \mathbf{u}_k^* and $\hat{\mathbf{u}}_{k+1}$, and assuming that there are no perturbations
 412 nor linearization errors, it can be shown that

413
$$\hat{\mathcal{J}}(k+1) - \mathcal{J}^*(k) = -x_{k|k}^T Q x_{k|k} - u_{k|k}^* R u_{k|k}^*, \quad (25)$$

414 where $\hat{\mathcal{J}}(i)$ and $\mathcal{J}^*(i)$ denote the values of the cost function for $\hat{\mathbf{u}}_i$ and \mathbf{u}_i^* ,
 415 respectively. As the RHS of (25) is semi-negative definite, then

416
$$\hat{\mathcal{J}}(k+1) \leq \mathcal{J}^*(k). \quad (26)$$

417 But $\hat{\mathbf{u}}_{k+1}$ is a feasible but sub-optimal sequence, then it can be said that
 418 $\mathcal{J}^*(k+1) \leq \hat{\mathcal{J}}(k+1)$, and consequently

419
$$\mathcal{J}^*(k+1) \leq \mathcal{J}^*(k) \quad \forall k. \quad (27)$$

420 This shows that the sequence of optimal cost values $\{\mathcal{J}^*(k)\}$ decreases along
 421 closed-loop trajectories of the system. The cost is bounded below by zero
 422 and thus has a nonnegative limit. Therefore as $k \rightarrow \infty$ the difference of
 423 optimal cost $\Delta \mathcal{J}^*(k+1) = \mathcal{J}^*(k+1) - \mathcal{J}^*(k) \rightarrow 0$. Because Q and R are
 424 positive definite, as $\Delta \mathcal{J}^*(k+1) \rightarrow 0$ the states and the inputs must converge
 425 to the origin $x_k \rightarrow 0$ and $u_k \rightarrow 0$ as $k \rightarrow \infty$.

426 *Stability.* To prove that the origin is asymptotically stable, from (27) it is
 427 clear that the sequence of optimal costs $\{\mathcal{J}^*(k)\}$ is non-increasing, which
 428 implies $\mathcal{J}^*(k) \leq \mathcal{J}^*(0) \forall k > 0$. At time $k = 0$, the cost function can be
 429 written as

$$430 \quad \mathcal{J}(0) = x_0^T P_0 x_0, \quad (28)$$

431 where P_0 satisfies the Lyapunov equation $P_k - A_k^T P_k A_k = Q$, $Q > 0$. From
 432 the definition of cost function, it can be written that

$$433 \quad x_k^T Q x_k \leq \mathcal{J}^*(k), \quad (29)$$

434 then,

$$435 \quad x_k^T Q x_k \leq \mathcal{J}^*(k) \leq \mathcal{J}^*(0) \leq \mathcal{J}(0) = x_0^T P_0 x_0, \quad (30)$$

436 which implies

$$437 \quad x_k^T Q x_k \leq x_0^T P_0 x_0 \quad \forall k. \quad (31)$$

438 Since Q and P_0 are positive definite it follows that

$$439 \quad \lambda \min(Q) \|x_k\|^2 \leq \lambda \max(P_0) \|x_0\|^2 \quad \forall k, \quad (32)$$

440 where $\lambda \min(\cdot)$ and $\lambda \max(\cdot)$ denote the min-max eigenvalue of the correspond-
 441 ing matrix. Finally it can be written that

$$442 \quad \|x_k\| \leq \sqrt{\frac{\lambda \max(P_0)}{\lambda \min(Q)}} \|x_0\| \quad \forall k > 0. \quad (33)$$

443 Thus, the closed-loop is stable. The combination of convergence and stabil-
 444 ity implies that the origin is asymptotically stable equilibrium point of the
 445 closed-loop system. \square

446 B. Proof of Theorem 2

447 *Proof.* As the cost function (12) is locally convex at each sampling instant
 448 and only linear inputs constraints are considered, the optimization problem
 449 of Algorithm 1 is locally convex.

450 Let the control input sequence \mathbf{u}_k^0 be a feasible solution at time k defined
 451 as:

$$452 \quad \mathbf{u}_k^0 = [u_{k|k-1}^*, u_{k+1|k-1}^*, \dots, u_{k+N-2|k-1}^*, 0]^T. \quad (34)$$

453 At time k , let \mathbf{u}_k be a feasible convex combination of \mathbf{u}_k^* and \mathbf{u}_k^0 , i.e.

454
$$\mathbf{u}_k = \alpha \mathbf{u}_k^* + (1 - \alpha) \mathbf{u}_k^0, \quad \text{with } 0 \leq \alpha \leq 1. \quad (35)$$

455 As $\mathcal{J}(k)$ is a locally convex function, it can be easily shown that

456
$$\begin{aligned} \mathcal{J}(k) &= \alpha \mathcal{J}^*(k) + (1 - \alpha) \mathcal{J}_0(k), \\ &= \alpha (\mathcal{J}^*(k) - \mathcal{J}_0(k)) + \mathcal{J}_0(k), \end{aligned} \quad (36)$$

457 as $0 \leq \alpha \leq 1$ and $\mathcal{J}^*(k)$ is the optimal value of the cost function at time k ,
 458 then

459
$$\alpha (\mathcal{J}^*(k) - \mathcal{J}_0(k)) \leq 0, \quad (37)$$

460 and consequently

461
$$\mathcal{J}(k) \leq \mathcal{J}_0(k), \quad (38)$$

462 This shows that at each time instant k the cost function $\mathcal{J}(k)$ is non-
 463 increasing, thus the resulting closed-loop is stable.

464

□

465 C. Proof of Theorem 3

466 *Proof.* At iteration $q = 1$ let \mathbf{u}_k^1 be a feasible convex combination of \mathbf{u}_k^* and
 467 \mathbf{u}_k^0 , i.e.

468
$$\mathbf{u}_k^1 = \alpha \mathbf{u}_k^* + (1 - \alpha) \mathbf{u}_k^0, \quad \text{with } 0 \leq \alpha \leq 1. \quad (39)$$

469 As the iterated cost function

470
$$\mathcal{J}^q(k) = \sum_{i=0}^{N-1} \left[\tilde{x}_{k+i|k}^{qT} Q \tilde{x}_{k+i|k}^q + \tilde{u}_{k+i|k}^{qT} R \tilde{u}_{k+i|k}^q \right] + \tilde{x}_{k+N|k}^{qT} P_{k|k}^q \tilde{x}_{k+N|k}^q, \quad (40)$$

471 is a locally convex function, then following a similar reasoning to the proof
 472 of Theorem 2, it can be easily shown that

473
$$\mathcal{J}^1(k) \leq \mathcal{J}^0(k), \quad (41)$$

474 The same argument can be repeated at subsequent iteration to show that

475
$$\mathcal{J}^{q+1}(k) \leq \mathcal{J}^q(k), \quad q \geq 0, \quad (42)$$

476 This shows that the sequence $\{\mathcal{J}^q(k)\}$ is non-increasing. As the cost function
 477 is quadratic, it is bounded below by zero and thus has a non-negative limit.
 478 Therefore, as $q \rightarrow \infty$ the difference of cost $\Delta \mathcal{J}^q(k) = \mathcal{J}^{q+1} - \mathcal{J}^q \rightarrow 0$, and
 479 as a result $\mathcal{J}^q(k) \rightarrow \mathcal{J}^*(k)$. □

480 D. Non-linear Quadcopter Model

481 The quadcopter state vector x is defined as:

$$482 \quad x = [n e h u v w \phi \theta \psi p q r]^T, \quad (43)$$

483 where n , e and $h = -z$ are the coordinates of the quadcopter CG position,
 484 u , v and w are the components of the quadcopter velocity vector, ϕ , θ and
 485 ψ are the Euler angles that define the roll, pitch and yaw movements and p ,
 486 q and r are the components of the quadcopter angular velocity vector. The
 487 quadcopter control inputs vector u is defined as:

$$488 \quad u = [\Omega_0 \Omega_1 \Omega_2 \Omega_3]^T, \quad (44)$$

489 where Ω_i denotes the absolute angular speed of the i -th rotor.

490 Defining c_α , s_α , and t_α as the notation representing $\cos(\alpha)$, $\sin(\alpha)$ and
 491 $\tan(\alpha)$, respectively, for a generic angle α , the 6-degrees of freedom (6-DOF)
 492 non-linear dynamic of a quadcopter can be represented by the following set
 493 of differential equations:

$$\dot{x} = \begin{bmatrix} u c_\theta c_\psi + v(s_\phi s_\theta c_\psi - c_\phi s_\psi) + w(c_\phi s_\theta c_\psi + s_\phi s_\psi) \\ u c_\theta s_\psi + v(s_\phi s_\theta s_\psi + c_\phi c_\psi) + w(c_\phi s_\theta s_\psi - s_\phi c_\psi) \\ u s_\theta - v s_\phi c_\theta - w c_\phi c_\theta \\ rv - qw - g s_\theta - \frac{\mu}{m} u - \frac{C A_x \rho}{2m} u |u| \\ pw - ru + g s_\phi c_\theta - \frac{\mu}{m} v - \frac{C A_y \rho}{2m} v |v| \\ qu - pv + g c_\phi c_\theta - \frac{b}{m}(\Omega_0^2 + \Omega_1^2 + \Omega_2^2 + \Omega_3^2) - \frac{C A_z \rho}{2m} w |w| \\ p + q s_\phi t_\theta + r c_\phi t_\theta \\ q c_\phi - r s_\phi \\ q s_\phi \sec \theta + r c_\phi \sec \theta \\ \frac{I_y - I_z}{I_x} qr + \frac{db\sqrt{2}}{2I_x}(-\Omega_0^2 - \Omega_1^2 + \Omega_2^2 + \Omega_3^2) - \frac{k\rho A}{I_x} p + \frac{J_r}{I_x} q(\Omega_0 - \Omega_1 + \Omega_2 - \Omega_3) \\ \frac{I_z - I_x}{I_y} pr + \frac{db\sqrt{2}}{2I_y}(\Omega_0^2 - \Omega_1^2 - \Omega_2^2 + \Omega_3^2) - \frac{k\rho A}{I_y} q - \frac{J_r}{I_y} p(\Omega_0 - \Omega_1 + \Omega_2 - \Omega_3) \\ \frac{I_x - I_y}{I_z} pq + \frac{\epsilon}{I_z}(\Omega_0^2 - \Omega_1^2 + \Omega_2^2 - \Omega_3^2) - \frac{k\rho A}{I_z} r + \frac{J_r}{I_z}(\dot{\Omega}_0 - \dot{\Omega}_1 + \dot{\Omega}_2 - \dot{\Omega}_3) \end{bmatrix}, \quad (45)$$

494 where \dot{x} is the time derivative of Eq. (43), $g = 9.81$ [m/sec] is the acceleration
 495 of gravity, $m = 1$ [kg] is the mass of the quadcopter, $I_x = 8.1 \cdot 10^{-3}$ [Nm sec²],
 496 $I_y = 8.1 \cdot 10^{-3}$ [Nm sec²] and $I_z = 14.2 \cdot 10^{-3}$ [Nm sec²] are the body moment
 497 of inertia around the x , y and z axis, respectively, $\mu = 1 \cdot 10^{-5}$ [kg/sec] is
 498 the rotor drag coefficient, $C = 3 \cdot 10^{-4}$ is a dimensionless friction constant,
 499 $A_x = 0.05$ [m²], $A_y = 0.05$ [m²] and $A_z = 0.1$ [m²] are the projections of
 500

501 the vehicle area on the yz , xz and xy planes of the B-Frame, respectively,
502 $\rho = 1.2$ [kg/m³] is the air density, $b = 54.2 \cdot 10^{-6}$ [N sec²] is the aerodynamic
503 contribution of thrust, $d = 0.24$ [m] is the distance between the center of the
504 quadcopter and the center of a propeller, $k = 1 \cdot 10^{-5}$ [m³/sec] is a frictional
505 constant, $A = 0.2$ [m²] is the vehicle area, $J_r = 104 \cdot 10^{-6}$ [Nm sec²] is the
506 rotational inertia of a propeller and $\epsilon = 1.1 \cdot 10^{-6}$ [Nm sec²] is a yaw drag
507 factor.

508 9. References

- 509 [1] J. Maciejowski, Predictive control: with constraints, Prentice Hall, 2002.
- 510 [2] J. Rawlings, D. Mayne, Model Predictive Control: Theory and Design,
511 Nob Hill Pub., 2009.
- 512 [3] K. Alexis, G. Nikolakopoulos, A. Tzes, Model predictive quadrotor con-
513 trol: attitude, altitude and position experimental studies, Control The-
514 ory Applications, IET 6 (12) (2012) 1812–1827. doi:10.1049/iet-cta.
515 2011.0348.
- 516 [4] S. Vazquez, J. Leon, L. Franquelo, J. Rodriguez, H. Young, A. Marquez,
517 P. Zanchetta, Model predictive control: A review of its applications in
518 power electronics, Industrial Electronics Magazine, IEEE 8 (1) (2014)
519 16–31. doi:10.1109/MIE.2013.2290138.
- 520 [5] A. Marasco, S. Givigi, C. Rabbath, Model predictive control for the dy-
521 namic encirclement of a target, in: American Control Conference (ACC),
522 2012, 2012, pp. 2004–2009. doi:10.1109/ACC.2012.6315602.
- 523 [6] M. Abdolhosseini, Y. Zhang, C. Rabbath, An efficient model pre-
524 dictive control scheme for an unmanned quadrotor helicopter, Jour-
525 nal of Intelligent & Robotic Systems 70 (1-4) (2013) 27–38. doi:
526 10.1007/s10846-012-9724-3.
- 527 [7] Y. Lee, B. Kouvaritakis, M. Cannon, Constrained receding horizon pre-
528 dictive control for nonlinear systems, Automatica 38 (12) (2002) 2093–
529 2102. doi:10.1016/S0005-1098(02)00133-4.
- 530 [8] M. Diehl, H. Ferreau, N. Haverbeke, Efficient numerical methods for
531 nonlinear mpc and moving horizon estimation, Nonlinear Model Predic-
532 tive Control (2009) 391–417doi:10.1007/978-3-642-01094-1_32.

- 533 [9] R. Lopez-Negrete, F. J. DAmato, L. T. Biegler, A. Kumar, Fast non-
534 linear model predictive control: Formulation and industrial process
535 applications, *Computers & Chemical Engineering* 51 (2013) 55 – 64.
536 doi:http://dx.doi.org/10.1016/j.compchemeng.2012.06.011.
- 537 [10] L. Biegler, X. Yang, G. Fischer, Advances in sensitivity-based nonlinear
538 model predictive control and dynamic real-time optimization, *Journal*
539 *of Process Control* 30 (2015) 104 – 116. doi:http://dx.doi.org/10.
540 1016/j.jprocont.2015.02.001.
- 541 [11] M. Morari, J. H. Lee, Model predictive control: past, present and future,
542 *Computers & Chemical Engineering* 23 (4-5) (1999) 667–682. doi:10.
543 1016/S0098-1354(98)00301-9.
- 544 [12] A. Brooms, B. Kouvaritakis, Successive constrained optimization and
545 interpolation in non-linear model based predictive control, *International*
546 *journal of control* 73 (4) (2000) 312–316. doi:10.1080/
547 002071700219669.
- 548 [13] W. C. Li, L. T. Biegler, A multistep, newton-type control strategy
549 for constrained, nonlinear processes, in: *American Control Conference*,
550 1989, IEEE, 1989, pp. 1526–1527.
- 551 [14] N. De Oliveira, Newton-type algorithms for nonlinear constrained chemical
552 process control, Ph.D. thesis, Carnegie Mellon University (1994).
- 553 [15] N. De Oliveira, L. Biegler, An extension of newton-type algorithms for
554 nonlinear process control, *Automatica* 31 (2) (1995) 281–286. doi:http://
555 dx.doi.org/10.1016/0005-1098(94)00086-X.
- 556 [16] D. Q. Mayne, J. B. Rawlings, C. V. Rao, P. O. Scokaert, Constrained
557 model predictive control: Stability and optimality, *Automatica* 36 (6)
558 (2000) 789–814. doi:10.1016/S0005-1098(99)00214-9.
- 559 [17] T. Yang, E. Polak, Moving horizon control of nonlinear systems
560 with input saturation, disturbances and plant uncertainty, *International*
561 *Journal of Control* 58 (4) (1993) 875–903. doi:10.1080/
562 00207179308923033.
- 563 [18] S. De Oliveira Kothare, M. Morari, Contractive model predictive control
564 for constrained nonlinear systems, *IEEE Transactions on Automatic*

- 565 Control 45 (6) (2000) 1053–1071. doi:10.1109/9.863592.
566 URL [http://ieeexplore.ieee.org/lpdocs/epic03/wrapper.htm?](http://ieeexplore.ieee.org/lpdocs/epic03/wrapper.htm?arnumber=863592)
567 [arnumber=863592](http://ieeexplore.ieee.org/lpdocs/epic03/wrapper.htm?arnumber=863592)
- 568 [19] P. Falcone, M. Tufo, F. Borrelli, J. Asgari, H. Tseng, A linear time
569 varying model predictive control approach to the integrated vehicle
570 dynamics control problem in autonomous systems, in: Decision and
571 Control, 2007 46th IEEE Conference on, IEEE, 2007, pp. 2980–2985.
572 doi:10.1109/CDC.2007.4434137.
- 573 [20] P. Falcone, F. Borrelli, H. E. Tseng, J. Asgari, D. Hrovat, Linear time-
574 varying model predictive control and its application to active steering
575 systems: Stability analysis and experimental validation, International
576 journal of robust and nonlinear control 18 (8) (2007) 862–875. doi:
577 10.1002/rnc.1245.
- 578 [21] W. Langson, I. Chrysochoos, S. Raković, D. Mayne, Robust model
579 predictive control using tubes, Automatica 40 (1) (2004) 125–133. doi:
580 10.1016/j.automatica.2003.08.009.
- 581 [22] F. A. Cuzzola, J. C. Geromel, M. Morari, An improved approach for con-
582 strained robust model predictive control, Automatica 38 (7) (2002) 1183
583 – 1189. doi:[http://dx.doi.org/10.1016/S0005-1098\(02\)00012-2](http://dx.doi.org/10.1016/S0005-1098(02)00012-2).
584 URL [http://www.sciencedirect.com/science/article/pii/](http://www.sciencedirect.com/science/article/pii/S0005109802000122)
585 [S0005109802000122](http://www.sciencedirect.com/science/article/pii/S0005109802000122)
- 586 [23] D. Q. Mayne, E. C. Kerrigan, E. J. van Wyk, P. Falugi, Tube-based
587 robust nonlinear model predictive control, International Journal of Ro-
588 bust and Nonlinear Control 21 (11) (2011) 1341–1353. doi:10.1002/
589 rnc.1758.
- 590 [24] M. Cannon, J. Buerger, B. Kouvaritakis, S. Rakovic, Robust Tubes in
591 Nonlinear Model Predictive Control, IEEE Transactions on Automatic
592 Control 56 (8) (2011) 1942–1947. doi:10.1109/TAC.2011.2135190.
- 593 [25] S. Yu, C. Maier, H. Chen, F. Allgöwer, Tube mpc scheme based
594 on robust control invariant set with application to lipschitz nonlinear
595 systems, Systems and Control Letters 62 (2) (2013) 194–200. doi:
596 10.1016/j.sysconle.2012.11.004.
597 URL <http://dx.doi.org/10.1016/j.sysconle.2012.11.004>

- 598 [26] J. A. Martínez, Model order reduction of nonlinear dynamic systems using
599 multiple projection bases and optimized state-space sampling, Ph.D.
600 thesis, University of Pittsburgh (2009).
- 601 [27] S. Rakovic, D. Mayne, Set robust control invariance for linear discrete
602 time systems, in: Decision and Control, 2005 and 2005 European Control
603 Conference. CDC-ECC '05. 44th IEEE Conference on, 2005, pp. 975–
604 980. doi:10.1109/CDC.2005.1582284.
- 605 [28] J. R. Cueli, C. Bordons, Iterative nonlinear model predictive control.
606 Stability, robustness and applications, Control Engineering Practice
607 16 (9) (2008) 1023–1034. doi:10.1016/j.conengprac.2007.11.003.
- 608 [29] J. B. Rawlings, K. R. Muske, The stability of constrained receding hori-
609 zon control, Automatic Control, IEEE Transactions on 38 (10) (1993)
610 1512–1516. doi:10.1109/9.241565.